

ELECTRIC FIELD STRENGTH IN A VORTEX-STABILIZED ARC

G. Yu. Dautov and M. I. Sazonov

Zhurnal Prikladnoi Mekhaniki i Tekhnicheskoi Fiziki, Vol. 8, No. 4, pp. 127-131, 1967

This paper is a continuation of [1], which was devoted to measurement of the axial component of the electric field in an arc stabilized by a vortical flow of gas and to generalization of the experimental data.

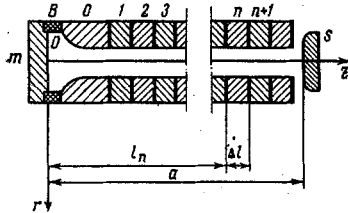


Fig. 1. Plasmatron with segmented channel.

1. Experimental apparatus, measurements, and generalization of results. We carried out the measurements by using a segmented

channel and by varying the interelectrode gap. The method of conducting the experiments was described in [1, 2]. Figure 1 shows a diagram of the plasmatron on which the measurements were made with a segmented channel. Its main components are the water-cooled electrodes *m* and *s* and the segments 0, 1, 2, ..., which are insulated from one another. Air was delivered through tangential apertures in the twist ring *B*, which is situated between the electrode *m* and segment 0. In the experiments in which the segment potentials were measured with an electrostatic voltmeter the segments were cooled with air. In this case the electric field strength *E* was determined from the slope of the curve of potential distribution along the *z*-axis. To determine *E* by the second method we varied the interelectrode gap *a* by altering the number of segments. The measurements were made on a length $l_1 < z < a$. The thickness Δl of the segments, the diameters *d* of the arc chamber, the ranges of variation of the current *I*, the flow rate *G*, the pressures *p* in the gas stream at the end of the channel, and the values of *a* and l_1 are given in the table.

It should be noted that, with the same *I*, *G*, *p*, *d*, and l_n within the limits of error of their measurement, the segment potentials changed in prolonged operation owing to the formation of a crater in the electrode *m*. These changes did not exceed ± 7 V. Such changes, however, did not affect the value of *E*, since the derivative of the potential distribution along *z* remained constant. In a number of cases we avoided these changes by changing the electrode *m* more frequently.

According to [3, 4], the general relationship for the electric field strength in arcs burning in plasmatrons of the type indicated can be put in the form

$$Ed = f(I/d, G/d, pd, a/d, z/d). \quad (1.1)$$

Below we give a general relationship for geometrically similar arc chambers, where *a/d* is constant and is contained as a constant in the general formula. It was shown in [1] that under certain conditions the variation of *E* with *z* is slight over a considerable length of the column and can be neglected. Experiments showed that for the tabulated range of parameters these conditions are satisfied when $z/d < 15$. Hence, for the generalization of these data formula

(1.1) can be simplified:

$$Ed = f(I/d, G/d, pd). \quad (1.2)$$

For a limited range of parameters variation (1.2) can be written in the form

$$Ed = c(G/d)^{\beta}(pd)^{\gamma}(c_0 + c_1 I/d + c_2 I^2/d^2). \quad (1.3)$$

In [1] for $d = 1.04$ cm, $p = 10$ N/cm², and $4 < a < 15$ cm we obtained the formula

$$E = -3.55 \cdot 10^{-3} G^{0.15} (5160 - 14.8 I + 0.073 I^2) \text{ [V/cm]} \quad (1.4)$$

where $[G] = \text{g sec}^{-1}$, $[I] = \text{A}$.

After the determination of γ the reverse transformation from (1.4) to the more general formula (1.3) gives

$$E = -4.21 \cdot 10^{-2} \varphi \text{ [V/cm]},$$

$$\varphi = G^{0.15} p^{0.18} d^{-1.02} (355 - I/d + 5.13 \cdot 10^{-3} I^2/d^2) \quad (1.5)$$

<i>d</i> = 0.5	1—1.04	2	2	2	3	cm
Δl = 0.5	0.75—1.2	1	1	1	2	cm
<i>I</i> = 70	40—170	70—100	70—180	70—220	70—180	<i>a</i>
<i>G</i> = 1.5	6—12	4	8—16	20	8—24	g sec^{-1}
<i>p</i> = 10	10—20	10	10—40	10	10	g sec^{-1}
l_1 = 1.3	4	3	3	3	1.5	cm
<i>a</i> = 7.5—9	15	30	30	30	45	cm

It is of interest to compare formula (1.5), obtained for one diameter of arc chamber, with the experimental data for other diameters. In Fig. 2 the solid line is given by formula (1.5), while the experimental points 1, 2, 3, and 4 correspond to diameters, 3, 2, 1, and 0.5 cm for the tabulated ranges of parameters. It is apparent that there is a satisfactory agreement between the formula and experiment for other values of *d* also. Thus, even a very limited amount of experimental data, treated by means of dimensional complexes corresponding to the variable parts of dimensionless criteria, gives useful information about the properties of the arc in a wider range of variation of the parameters.

In the present work the value of γ was found from data obtained for a small range of variation of *p*. Hence its verification will require experiments involving variation of *p* by an order, at least.

2. Connection between segment potential and arc potential. A question which naturally arises is that of the cross section of the arc to which the segment potential relates. This question was considered in [5-7] for the case in which a cylindrical arc almost completely filled the arc chamber and the segments operated as probes.

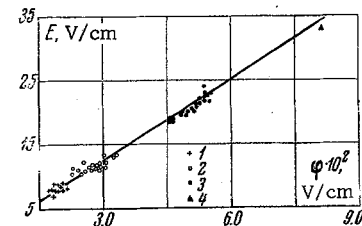


Fig. 2. Comparison of formula (1.5) with experiment.

In the case of plasmatrons in which there is a considerable layer of cold gas between the wall of the chamber and the column, the conditions of operation of the segment differ considerably from probe conditions and require special consideration. For this purpose we carried out the following experiments.

a) In the case of direct polarity of the plasmatron (*m* the cathode, *s* the anode) and $d = 2$ cm the segment for which $\Delta l = 1$ cm and

$l_n = 15.5$ cm was replaced by five segments 0.15 cm thick (0.2 cm including the insulator). Points 2 in Fig. 3 show the potentials of these thin segments for $I = 100$ A, $G = 8.1$ g sec⁻¹, and $a = 29.2$ cm, while points 1 show the potentials of segments with $\Delta l = 1$ cm for the same values of I and G . Points 1 on the graph are assigned to the midsections of the segments. As the figure shows, points 2 lie satisfactorily on the potential distribution line determined by means of segments 1 cm thick. Hence, we can conclude that in the experiments the segment potential was equal to the arc potential in the middle cross section of the segment.

b) The validity of this conclusion for direct polarity of the plasmatron was confirmed by measurement of the potential of electrically connected segments $n, n + 1, n + 2, n + 3, n + 4$, with $l_n = 19.4$ cm, $\Delta l = 1$ cm, $d = 2$ cm, $I = 100$ A, $G = 82$ g sec, and $a = 29.2$ cm.

Point 2 in Fig. 4 shows the potential of the connected segments, and point 1 shows the potentials of these segments before connection. There is a good agreement between point 2 and the potential of the midsection. Thus, even when $\Delta l = 5$ cm, the segment potential is equal to the arc potential in the mid section. The experimental electric-field-strength data for the generalization were obtained for the case of direct polarity and, hence, the measured potentials related to the midsections of the segments.

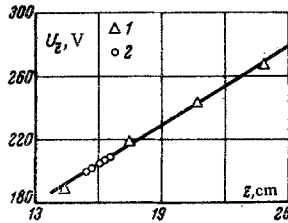


Fig. 3. Potential distribution in direct polarity case.

c) Similar experiments were performed with a plasmatron of reverse polarity (m is the anode and s is the cathode). Points 3 in Fig. 4 show the potentials of five segments insulated from one another, while point 4 is the potential of the same segments when they were connected. In this case the potential of the connected segments differed appreciably from the potential of the midsection. This deviation can be explained by consideration of the volt-ampere characteristics of the independent discharge between the arc column and the segments.

d) In the experiments the voltage on a length of arc column equal to the thickness of the segments was 10–30 V. Hence, when the potential distribution along the arc is linear, the potentials of adjacent segments differ by the same amount. We had to find out if the potential of the segments was affected by the neighboring segments when such potential differences existed. To test this we connected the segment with $\Delta l = 1$ cm, $l_n = 24.5$ cm ($I = 182$ A, $G = 20$ g sec and direct polarity of the plasmatron) to the anode, i. e., we applied a potential of about 600 V, whereas its floating potential

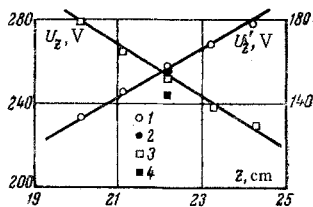


Fig. 4. Comparison of potentials of insulated and connected segments.

(i. e., the potential of the insulated segment) was 285 V. Connection of the segment to the anode did not affect the potentials of the adjacent segments. Thus, as in the case of a cylindrical arc [6], disturbance of the segment potential owing to the effect of adjacent segments can be neglected.

3. Independent discharge. The volt-ampere characteristics of an independent discharge between the arc and the segments revealed

some special features of the operation of the segments and the method of measuring the arc potential. Figure 5 shows the volt-ampere characteristics $U_m(i)$ of this discharge of two segments $l_n = 16.3$ cm and $l_n = 23.6$ cm with $d = 2$ cm and $\Delta l = 1$ cm. The potential drop on the independent discharge (difference in potential of seg-

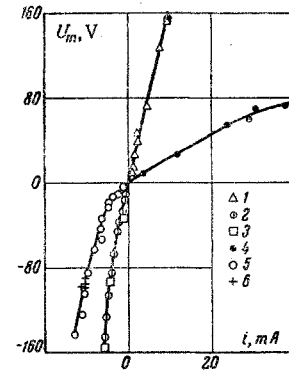


Fig. 5. Volt-ampere characteristics of independent discharge between arc and segments with $I = 100$ A, $a = 29.2$ cm. 1), 2), 3) $l_n = 16.3$ cm; 4), 5), 6) $l_n = 23.6$ cm.

ment and arc at the midsection of the segment) is plotted on the y-axis and i is the current through the subject segment. The direction from the segment to the arc was taken as the positive direction of i . These experiments were carried out with direct and reverse polarities of the plasmatron. In the case of direct polarity the regions of the volt-ampere characteristics of the discharge for $U_m > 0$ (point 1, 4) were obtained by altering the resistance between the segment and the anode, and in the case $U_m < 0$ (points 2, 5) by application of a voltage to the segment by a UIP-1 power supply. The volt-

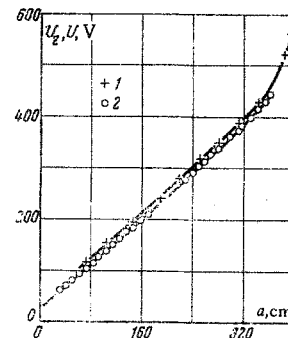


Fig. 6. Plot of arc voltage against arc length (curve 1) and potential distribution (curve 2) for $I = 140$ A, $G = 12.1$ g sec⁻¹, $d = 2$ cm, and direct polarity.

ampere characteristics in the case of reverse polarity of the plasmatron (points 3, 6) were obtained by altering the resistance between the segment and the cathode. The figure shows that the volt-ampere characteristics for direct and reverse polarity coincide.

One of the special features of these characteristics in comparison with the volt-ampere characteristics of segments operating as probes ([5], for instance) is the much smaller current for the same potential drop, while the volt-ampere characteristic of the segment $l_n = 16.3$ cm is not at all like the probe characteristic, even in general form.

Figure 5 also shows that for segment $l_n = 16.3$ cm with -30 V $< U_m < 160$ V and for segment $l_n = 23.6$ cm with -6 V $< U_m < 10$ V the volt-ampere characteristics are almost linear. We will consider the discharge between segment $l_n = 16.3$ cm and the arc column. When $d = 2$ cm for the tabulated range of parameters we have $E = 10$ –12 V/cm and, hence, the potential drop on the part of the arc within a segment 1 cm thick is 10–12 V. Owing to this, the difference in the floating potential of the segment and the arc potential

at any cross section within the thickness of the segment does not exceed 10–12 V in absolute value. Hence, the volt-ampere characteristics of the discharge between elements of the segment and the

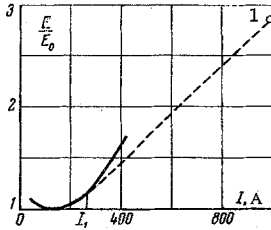


Fig. 7. Relative electric field strength as a function of current.

arc will be linear, and the floating potential of the segment will be equal to the arc potential in the midsection of the segment. A comparison of the volt-ampere characteristics shows that with increase in l_n their linear regions near the coordinate origin become smaller. Hence, in the case of large l_n the thickness of the segment must be small if the floating potential is to be equal to the arc potential at the mid section of the segment. Otherwise the segment acquired the potential of the arc in a section away from the middle. We know that when a channel segment of a cylindrical arc operated as a probe, it usually acquired the potential of the arc in a section close to the end of the segment [5]. Thus, despite the high flow rate, at large values of l_n the behavior of the floating potential of a segment of the electric-arc chamber of a plasmatron is similar to that in [5–7]. This is quite understandable, since the thickness of the layer of cold gas between the arc column and the chamber wall decreases with increase in l_n .

We turn now to an explanation of the results of Fig. 4. We use the following properties of the volt-ampere characteristics shown in Fig. 5: 1) when $U_m = \text{const}$, i increases with increase in l_n ; 2) for the same values of l_n , if $|U_m'| = |U_m''|$, $U_m' > 0$, $U_m'' < 0$, then $|i'| \geq |i''|$.

We consider the case of direct polarity where the segments n , $n+1$, $n+2$, $n+3$, and $n+4$ are connected. For the sections n , $n+1$ we have $U_m > 0$, and for segments $n+3$, $n+4$ we have $U_m < 0$. In addition, l_{n+3} and l_{n+4} are greater than l_n and l_{n+1} . In view of these properties of the volt-ampere characteristics the currents through segments $n+3$ and $n+4$ are affected in opposite ways by the negativity of U_m and the greater distances of these segments from the electrode m ; these factors compensate one another. Hence, the potential of the five connected segments is equal to the potential of the central segment.

In the case of reverse polarity these factors act in the same way and, hence the density of the positive currents through the last segments is greater. Thus, the cross section with zero current density, where the potentials of the arc and the connected segments are equal, is shifted in the direction of the flow.

4. Effect of arc length and current on electric field strength.

Experiments showed that an increase in interelectrode gap a and, hence, in arc length, affected the value of E in several ways. First, beginning at a certain value of a the distribution of potential U_z along the z -axis ceased to be linear (Fig. 6). The deviation from linearity occur earlier, the greater I and the smaller G .

Secondly, an increase in a with I , G , p , and d constant leads to an increase in the amount of heat supplied to the gas. Hence,

the temperature of the gas at the outlet of the arc chamber is increased, and the pressure in a fixed cross section $z = \text{const}$ is increased. For instance, the pressure in the cross section $z = a_1$ with constant pressure p in the gas stream at the outlet of the arc chamber increased from p to p_1 , with increase in a from a_1 to a_2 . Hence, on the linear portion of the change in U_z with increase of a from a_1 to a_2 the field strength in the cross section $z = a_1$ increases owing to the increase in pressure.

Formula (1.5) was obtained by generalization of the data for $I < 220$ A, $25 < I/d < 180$ A/cm. In this formula the numerical values of the coefficients c_0 , c_1 , and c_2 depend on I/d , G/d , and pd , and the coefficients can be regarded as constant only in a limited range of variation of the latter quantities. It is of interest to assess the effect of I on E at large values of I/d . The relationship between the dimensionless quantity E/E_0 and I when $G = G_0$, $p = p_0$, $d = d_0$, and $a = a_0$ can be written in the form of $E/E_0 = \psi(I)$, where E_0 is the minimum valued of E when $I = I_0$. In the investigated range of variation of I/d we have

$$\psi(I) = (c_0 + c_1 I/d_0 + c_2 I^2/d_0^2)(c_0 + c_1 I_0/d_0 + c_2 I_0^2/d_0^2)^{-1}. \quad (4.1)$$

In Fig. 7 the solid curve is given by formula (4.1) for $d_0 = 1.4$ cm. The correctness of this curve has been verified up to $I/d = 180$ A/cm, which for $d_0 = 1.4$ cm corresponds to a current $I_1 = 250$ A. In the same conditions, according to the indirect data of an unpublished investigation by O. I. Yas'ko and A. I. Zhidovich, which was kindly presented to us, the electric field strength for a current of the order of 1000 A is approximately 70 V cm^{-1} , which corresponds to the point 1 indicated by the circle in Fig. 7. For a rough estimate of the value of E at high currents we can use the dashed line connecting point 1 and the point on the solid curve corresponding to $I_1 = 250$ A.

REFERENCES

1. G. Yu. Dautov, Yu. S. Dudnikov, M. F. Zhukov, and M. I. Sazonov, "Potential distribution along an arc in a vortex-type plasmatron," PMTF [Journal of Applied Mechanics and Technical Physics], no. 5, 1965.
2. G. Yu. Dautov, Yu. S. Dudnikov, and M. I. Sazonov, "Investigation of a plasmatron with an interelectrode insert," Izv. SO AN SSSR, no. 10, part 3, 1965.
3. G. Yu. Dautov and M. F. Zhukov, "Some generalizations of electric-arc investigations," PMTF [Journal of Applied Mechanics and Technical Physics], no. 2, 1965.
4. G. Yu. Dautov and M. F. Zhukov, "Critical generalization of characteristics of vortex-type plasmatrons," PMTF [Journal of Applied Mechanics and Technical Physics], no. 6, 1965.
5. H. Edels and C. W. Kimblin, "A technique for measurement of the electrical conductance of plasma columns," International Symposium on the Properties and Application of a Low-Temperature Plasma at the 20-th International Congress on Theoretical and Applied Chemistry, Moscow, 1967.
6. H. B. Mecke, R. C. Dean, A. Pytte, "Cooled anodes with arc-heated flow," IEEE Transactions on nuclear science, vol. NS-11, no. 1, 1964.
7. H. W. Emmons, R. I. Zand, "The Poiseuille plasma experiment," Phys. Fluids, vol. 5, no. 12, 1962.